Antarctic Elevation Change from 1992 to 1996

Duncan J. Wingham,* Andrew J. Ridout, Remko Scharroo, Robert J. Arthern, C. K. Shum

Satellite radar altimeter measurements show that the average elevation of the Antarctic Ice Sheet interior fell by 0.9 ± 0.5 centimeters per year from 1992 to 1996. If the variability of snowfall observed in Antarctic ice cores is allowed for, the mass imbalance of the interior this century is only −0.06 ± 0.08 of the mean mass accumulation rate.

The best estimate of 20th century sea-level rise is 1.8 mm year^{-1} (*1*). Of this, known sources are insufficient by 360 Gt year^{-1} of water (*1*). This missing water may reflect uncertainties in sea-level rise, ocean thermal expansion (*2*), change in the Greenland Ice Sheet (*3*) and other land ice (*4*), and groundwater storage (*5*). It could equally signal a source as large as 500 Gt year^{-1} within the grounded Antarctic Ice Sheet (*1*, *6*). However, one part of the grounded ice area (42%) has been estimated (*7*) from sparse glaciological data to be growing at 118 Gt year^{-1}. If this part is characteristic of the whole grounded ice sheet, Antarctica has been a 435 Gt year^{-1} sink of ocean mass (*7*).

Here we use 5 years of spatially continuous ERS satellite measurements to estimate the rate of change of thickness of 63% of the grounded Antarctic Ice Sheet. Between 1992 and 1996, 4 × 10^{6} ice-mode ranges were recorded by the ERS-1 and ERS-2 satellite altimeters (*8*) at crossing points of the satellites' orbit ground tracks. The ranges were corrected for the lag of the leading-edge tracker (*9*), surface scattering (*10*), dry atmospheric mass (*11*), water vapor (*11*), ionosphere (*11*), slope-induced error (*9*), solid Earth tide (*11*), ocean loading tide (*11*), and isostatic rebound (*12*). The satellite location was determined with the DGM-E04 orbit model (*13*). After data editing, we formed time series of 35-day averages of elevation change (Fig. 1). From these time series (*14*), we determined the average 5-year rate of elevation change for 1° by 1° cells (Fig. 2), the major drainage basins, and the entire region of coverage (ROC) (Table 1).

We also estimated the total error covariance (Fig. 3) of the elevation change by summing its contributions. For errors that decorrelate over less than 35 days, we determined the covariance of elevation rate that arose when crossover sums were replaced with differences (*14*). This method should account for the speckle-induced error and much of the atmospherically related and satellite-location errors. The variability was 4.10 cm year^{-1}, decorrelating to ~0.4 cm year^{-1} at separations larger than 200 km. For satellite-location errors with longer correlations, we examined the difference in elevation change that arose on replacing the satellite locations with those from the TEG-3 orbit model (*15*). These errors are negligible. We estimated that the variability due to instrument system drift was 0.13 cm year^{-1} by differencing the ice-free Southern Ocean elevations measured by the ERS and TOPEX/Poseidon (*16*) altimeters south of 50°S. Instrument changes (particularly to gain control in December 1992 and orbit altitude in April 1994 and March 1995) result in a residual error in the tracker-lag correction. By replacing the leading-edge tracker with echo cross correlation, we estimated that the variability of this error was 0.5 cm year^{-1}. We were unable to estimate from independent measurements a residual error in the surface-scattering correction. This correction is large in places, but were it substantially in error, we would expect to find correlation between the correction and the elevation rate. However, the largest correlation coefficient at any value of separation was 0.06.

Elevation changes corrected for isostatic rebound reflect thickness changes due to changes in ice flow, bottom melting, snow accumulation, and ablation. In the interior, bottom melting is small and few places experience net ablation. If we assume that in the interior, ice is flowing by internal shear over a frozen or rough bed, the flow is unlikely to have altered on century to millennial time scales. Accumulation since the middle of the 19th century (*17–23*) has fluctuated in the interior about a constant mean accumulation rate (MAR). A change in elevation should result from either a century-scale mass imbalance or a contemporary fluctuation in accumulation rate. (We assume a century scale because there are few records of accumulation before 1850.)

Accumulation fluctuations occur at annual to decadal scales (*17–23*) and will appear (*24*) in the elevation rate with the density of snow. Their 5-year point variability is ~0.15 of the MAR (hereafter 0.15 MAR) (*25*). The density of snow is ~350 kg m^{-3}; Table 1 gives the spatial average of MAR (hereafter $\overline{\text{MAR}}$). With these data, the average temporal variability of the fluctuation within the ROC is 5.5 cm year^{-1}. At any point, the total elevation error from satellite observation is similar. Its variability is 4.13 cm year^{-1} (Fig. 3). However, the elevation error decorrelates rapidly with distance (Fig. 3). For the ROC as a whole, it is 0.5 cm year^{-1}. The extent to which the elevation change can be used to estimate the century-scale imbalance at large scales depends on how snow accumulation has fluctuated with distance.

Accumulation has fluctuated greatly this century at ice-core sites in separate drainage basins in the Antarctic interior, and there seems to be little or no correlation among these sites (*26*). On the other hand, if a substantial covariability survives at 1° by 1° (~100 km by 30 km), it should be apparent in the measured elevation change. We compared the covariance of the measured elevation change with the total error covariance (Fig. 3). The difference between them is the actual covariance of the

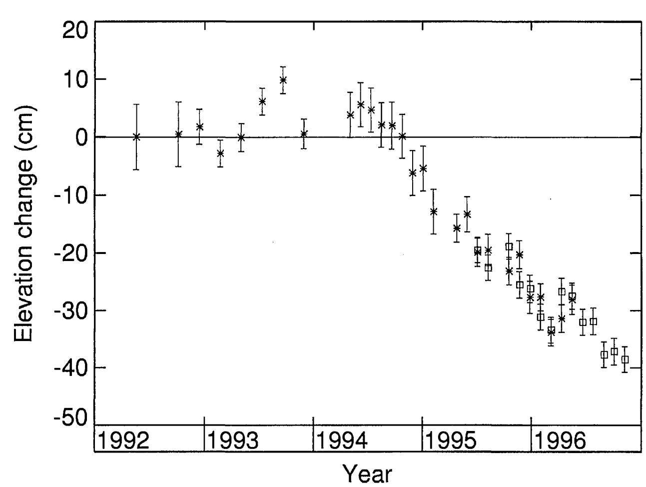

Fig. 1. The elevation change from 1992 to 1996 of basin G-H (Fig. 2). Simultaneous ERS-1 (stars) and ERS-2 (squares) observations were made from June 1995 to May 1996; the overlap allowed cross calibration. Data gaps result from instrument operation and are common to all basins.

D. J. Wingham, A. J. Ridout, R. J. Arthern, Department of Space and Climate Physics, University College London, 17-19 Gordon Street, London WC1H 0AH, UK. R. Scharroo, Delft Institute for Earth-Oriented Space Research, Delft University of Technology, Kluyverweg 1, 2629 HS Delft, Netherlands. C. K. Shum, Departments of Civil and Engineering Science and Geodetic Science, Ohio State University, 2070 Neil Avenue, Columbus, OH 43210, USA.

*To whom correspondence should be addressed.

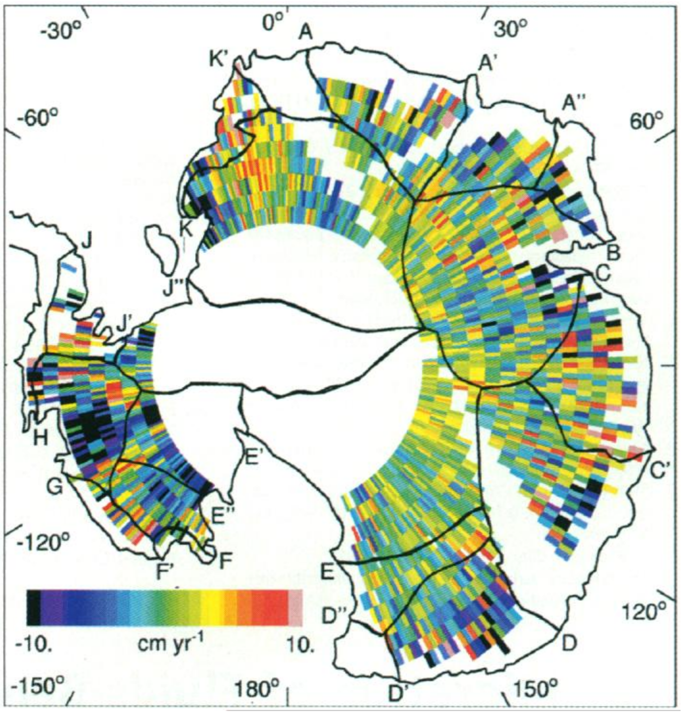

Fig. 2. The change in elevation from 1992 to 1996 (expressed in centimeters per year) of 63% of the grounded Antarctic Ice Sheet at a resolution of 1° by 1°, determined from ERS satellite altimeter measurements. Superimposed are the boundaries of the major drainage basins derived from ERS observations (*33*). The data gaps affecting basins K′-A, A′-A″, and C′-D result from tape-recorder limitations. The change of basin G-H appears to fall within the boundaries of the Thwaites Glacier Basin, and there is perhaps reason (*34*) to suppose that the Thwaites Glacier is drawing down its basin. However, the change in elevation of the basin is not unusual in comparison with the expected snowfall variability (Table 1). In addition, the change is unsteady (Fig. 1); a snowfall fluctuation is certainly implicated in the volume reduction.

elevation rate. The variability of the difference was 2.7 cm year^{-1}, and the correlation scale was ~200 km throughout the ROC. We therefore take $200^2\pi$ km^2 as the areal correlation scale for snow accumulation. To estimate (*27*) the variability of snowfall of a basin (Table 1), we assumed that the snowfall variance reduces as the ratio of the basin area to this reference area.

To estimate the century-scale imbalance, we treated the elevation change error and snowfall variability as equivalent sources of uncertainty. From Table 1, the estimated ice imbalances of individual basins range from 0.42 to −0.28 $\overline{\mathrm{MAR}}$; the average uncertainty is 0.30 $\overline{\mathrm{MAR}}$. For East Antarctica (basin J″-E′), the estimated imbalance is −1 ± 53 Gt year^{-1} or 0.00 ± 0.08 $\overline{\mathrm{MAR}}$; for West Antarctica (basin E′-J″), it is −59 ± 50 Gt year^{-1} or −0.17 ± 0.15 $\overline{\mathrm{MAR}}$; and for the ROC as a whole, it is −60 ± 76 Gt year^{-1} or −0.06 ± 0.08 $\overline{\mathrm{MAR}}$. This last value of imbalance has a lower uncertainty than the range of −0.28 to 0.24 $\overline{\mathrm{MAR}}$, which is equivalent to the −500 to 435 Gt year^{-1} that previous observations (*1*, *6*, *7*) allow for the grounded ice. Fifty gigatons per year equals 0.14 mm year^{-1} of eustatic sea-level change (*6*). It appears that the interior of the Antarctic Ice Sheet has been at most only a modest source or sink of sea-level mass this century. The data also provide evidence that the fluctuations in snowfall observed in the sparse Antarctic ice-core record (for example, *17*–*23*) are not characteristic of the continent but have a spatial scale of 200 km on average.

It is possible that a larger imbalance has been compensated for by a fluctuation in accumulation of the opposite sign that is larger than we estimate. The estimate of snowfall variability is made from observations (*25*) at locations outside the ROC that are not contemporary with the elevation change; the spatial scale of fluctuation may vary over the ice sheet, and the elevation change extends over one 5-year interval. Nonetheless, an imbalance of −0.28 or 0.24 $\overline{\mathrm{MAR}}$ makes a heavy demand on the contemporary snowfall. For example, an imbalance of −0.28 $\overline{\mathrm{MAR}}$ requires (*28*) that the accumulation increased throughout the ROC by greater than half the point variability (0.08 $\overline{\mathrm{MAR}}$). However, in general, recent accumulation in Antarctica does not look unusual. Between 1955 and 1996, accumulation has been high at some sites (*6*, *29*) and low (*18*) or close to the century mean (*6*, *18*, *22*, *23*, *30*) at others. Although a recent increase in mean annual Antarctic temperature has occurred (*29*), it is

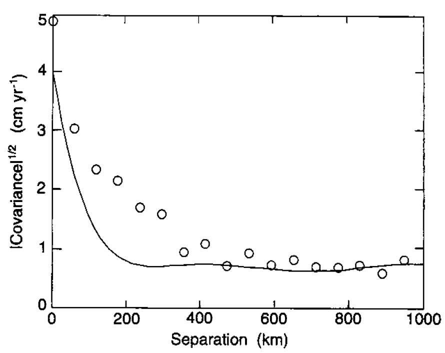

Fig. 3. The covariance of the measured 1992 to 1996 elevation rate (circles) of 63% of the grounded Antarctic Ice Sheet compared with the estimated total error covariance (solid line). The values at zero separation are the variances of the measured elevation rate (4.9^2 cm^2 year^{-2}) and its total error (4.13^2 cm^2 year^{-2}).

Table 1. The observed area, mean accumulation rate ($\overline{\mathrm{MAR}}$), estimated snowfall variability, and average elevation rate from 1992 to 1996 of Antarctic Ice Sheet drainage basins.

Drainage basin	Observed area* (10^6 km^2)	Mean ice accumulation rate† (cm year^{-1})	Snowfall variability‡ (cm year^{-1})	Average elevation rate (cm year^{-1})
J″-K	0.85	8	1.4	0.3 ± 0.7
K-K′	0.16	21	7.3	4.4 ± 1.1
K′-A	0.06	13	6.3	5.4 ± 1.4
A-A′	0.54	10	1.9	−1.1 ± 0.9
A′-A″	0.33	11	2.4	0.1 ± 0.8
A″-B	0.14	16	6.0	−2.7 ± 1.3
B-C	1.31	7	0.9	0.2 ± 0.8
C-C′	0.61	18	4.1	−0.6 ± 1.1
C′-D	0.75	15	3.1	−0.6 ± 0.7
D-D′	0.55	17	3.4	0.6 ± 1.0
D″-E	0.29	9	2.3	1.6 ± 0.7
E-E′	0.76	7	1.1	−1.0 ± 1.2
E′-E″	0.17	17	6.1	−0.5 ± 0.6
E″-F	0.25	16	4.7	−2.5 ± 0.9
F-F′	0.03	27	10.6	−3.3 ± 2.6
F′-G	0.08	31	12.2	6.7 ± 2.1
G-H	0.43	42	9.3	−11.7 ± 1.0
J-J′	0.17	46	16.2	−4.1 ± 1.8
J′-J″	0.08	22	8.6	−5.6 ± 1.3
J″-E′	6.4	11	0.8	0.0 ± 0.5
E′-J″	1.2	31	4.4	−5.3 ± 0.9
J″-J″	7.6	14	1.0	−0.9 ± 0.5

*Derived from the elevation model of (*33*). †Assumes 917 kg m^{-3} for the density of ice. Derived from (*32*). The values are accurate to perhaps 20%. ‡Assumes a density of snow of 350 kg m^{-3}. See (*27*).

too small to explain a fluctuation of ~0.25 $\overline{\mathrm{MAR}}$. A large century-scale imbalance for the Antarctic interior is unlikely. This conclusion is in keeping with a body of relative sea-level and geodetic evidence supporting the notion that the grounded ice has been in balance at the millennial scale (*31*).

References and Notes

1. R. Warrick, C. Le Provost, M. Meier, J. Oerlemans, P. Woodworth, in *Climate Change 1995: The Science of Climate Change* (Cambridge Univ. Press, Cambridge 1996), pp. 359–405. We use 1 mm year^{-1} of sea level = 360 Gt year^{-1} water (*6*).
2. V. Gornitz, *Earth Surf. Processes Landforms* **20**, 7 (1995).
3. N. Reeh, in *Glaciers, Ice Sheets and Sealevel: Effects of a CO_2 Induced Change* (National Academy Press, Washington, DC, 1985), pp. 155–171.
4. M. F. Meier, *Science* **226**, 1418 (1984).
5. B. Chao, *J. Geophys. Res.* **93**, 13811 (1988).
6. S. S. Jacobs, *Nature* **360**, 29 (1992).
7. C. R. Bentley and M. B. Giovinetto, in *Proceedings of the International Conference on the Role of Polar Regions in Global Change* (Univ. of Alaska, Fairbanks, AK, 1991), pp. 481–488. The authors obtained 400 Gt year^{-1} using 1660 Gt year^{-1} for the grounded ice accumulation. We used (*32*) 1811 Gt year^{-1} to get 435 Gt year^{-1}.
8. *ERS User Handbook* (ESA Publication SP-1148, European Space Agency, Noordwijk, Netherlands, 1993).
9. J. L. Bamber, *Int. J. Remote Sensing* **14**, 925 (1994).
10. R. J. Arthern, thesis, University of London (1997). Changes in surface backscatter result in spurious changes in elevation. For small changes, the relation is linear. The gradient is spatially variable because it depends on the volume scatter. We regressed the 1° by 1° elevation changes with power changes for June 1993 to December 1994. The average gradient was 0.38 m dB^{-1}. The correlation coefficient was almost everywhere higher than 0.7. We corrected the 5-year 1° by 1° time series by subtracting the product of the corresponding gradient and the power change. The correction ranges from −25.7 cm year^{-1} to 38.8 cm year^{-1} with a mean of 1.1 cm year^{-1} and a standard deviation of 6.11 cm year^{-1}.
11. W. Cudlip *et al.*, *Int. J. Remote Sensing* **14**, 889 (1994).
12. J. Wahr, *Geophys. Res. Lett.* **22**, 977 (1995).
13. R. Scharroo and P. N. A. M. Visser, *J. Geophys. Res.* **103**, 8113 (1998).
14. Within each 1° by 1° cell and 35-day interval centered at time t, there are ascending $a(t)$ and descending $d(t)$ range pairs. We formed $0.5\{[a(t_2) - d(t_1)] \pm [d(t_2) - a(t_1)]\}$. "+" gives the elevation change; "−" estimates errors that change within the 35-day averaging period (plus a time-invariant term). We formed basin time series from areally weighted averages of 1° by 1° time series of changes, with $t_1 \equiv$ April 1993. To form the total error variance for each time point, we summed the variances due to changes within 35 days, instrument system drift, and operation changes. The basin 35-day variance was the areally weighted average of 1° by 1° variances; other values are given in the text. We determined elevation rate and rate error by least squares fit of a linear trend to the time series, inversely weighted by the error variance.
15. C. K. Shum *et al.*, *Precise Orbit Analysis and Global Verification Results from ERS-1 Altimetry* (ESA Publication SP 361, European Space Agency, Noordwijk, Netherlands, 1994).
16. L.-L. Fu *et al.*, *J. Geophys. Res.* **99**, 24369 (1994).
17. A. Gow, *Technical Report 78* (Corps of Engineers, U.S. Army Cold Regions Research and Engineering Laboratory, Hanover, NH, 1961).
18. E. Isaksson *et al.*, *J. Geophys. Res.* **101**, 7085 (1996).
19. R. L. Cameron, in *Antarctic Snow and Ice Studies*, vol. 2 of *Antarctic Research Series*, M. Mellor, Ed. (American Geophysical Union, Washington, DC, 1964), pp. 1–31.
20. M. B. Giovinetto and W. Schwerdtfeger, *Arch. Meteorol. Geophys. Bioklimatol. Ser. A* **15**, 227 (1966).
21. R. M. Koerner, in *Antarctic Snow and Ice Studies II*, vol. 16 of *Antarctic Research Series* A. P. Crary, Ed. (American Geophysical Union, Washington, DC, 1971), pp. 225–238.
22. J. Petit, J. Jouzel, M. Pourchet, L. Merlivat, *J. Geophys. Res.* **87**, 4301 (1982).
23. E. Mosely-Thompson *et al.*, *J. Glaciol.* **37**, 11 (1991).
24. R. J. Arthern and D. J. Wingham, *Clim. Change*, in press. For an ice column, the thickness rate equals the mass imbalance divided by the density. However, because the near surface is snow densifying under its own weight, an accumulation fluctuation will appear in the thickness rate with an effective density lying between that of snow and ice that depends on the time scale of the fluctuation. In the interior, decadal and century fluctuations will appear with densities close to those of snow and ice, respectively. We use this "two-scale" approximation.
25. Given data are 0.15 MAR "short-term variability" (*20*). Values calculated from tabulated data are 0.03 MAR (*23*) and 0.11 MAR (*17*); values calculated from graphic data are 0.14 MAR (*19*), 0.17 MAR (*21*), and 0.19 MAR (*18*).
26. H. Enomoto, *Clim. Change* **18**, 67 (1991).
27. The temporal variability of the 5-year elevation rate from accumulation fluctuations is ~0.15 MAR/ρ_{snow}, where ρ_{snow} is the density of snow. Over a region large in comparison with the correlation scale, the spatial variability is ~0.15 $\sqrt{\overline{\mathrm{MAR}^2}}/\rho_{snow}$, where $\overline{\mathrm{MAR}^2}$ is the area average of MAR^2. The temporal variability (Table 1, column 4) of an area average of elevation rate is ~0.15 $\sqrt{\overline{\mathrm{MAR}^2}/n}/\rho_{snow}$, where n is the effective number of independent values of MAR within the region. We take $n \sim A/200^2\pi$, where A is the area in square kilometers. If $n < 1$, we set it equal to 1.
28. An ice imbalance of −0.28 $\overline{\mathrm{MAR}}$ is −3.9 cm year^{-1} in the ROC. The elevation rate is −0.9 cm year^{-1}, leaving 3.0 cm year^{-1} of snowfall fluctuation. This is equivalent to $3.0\rho_{snow}/\rho_{ice} = 1.15$ cm year^{-1} of ice, or 0.08 $\overline{\mathrm{MAR}}$ (where ρ_{ice} is the density of ice).
29. V. I. Morgan, I. D. Goodwin, D. M. Etheridge, C. W. Wookey, *Nature* **354**, 58 (1991).
30. C. Raymond *et al.*, *J. Glaciol.* **42**, 510 (1996).
31. W. R. Peltier, *Science* **240**, 895 (1988).
32. D. G. Vaughan, J. L. Bamber, M. B. Giovinetto, J. Russell, P. R. Cooper, *J. Clim.*, in press. We used their 1° by 1° values of MAR with the ROC mask (Fig. 2).
33. J. L. Bamber and P. Huybrechts, *Ann. Glaciol.* **23**, 364 (1996).
34. T. J. Hughes, *J. Glaciol.* **27**, 518 (1981).

35. This work was supported by the United Kingdom Natural Environment Research Council.

13 July 1998; accepted 20 August 1998

Migration of Fluids Beneath Yellowstone Caldera Inferred from Satellite Radar Interferometry

Charles Wicks Jr., Wayne Thatcher, Daniel Dzurisin

Satellite interferometric synthetic aperture radar is uniquely suited to monitoring year-to-year deformation of the entire Yellowstone caldera (about 3000 square kilometers). Sequential interferograms indicate that subsidence within the caldera migrated from one resurgent dome to the other between August 1992 and August 1995. Between August 1995 and September 1996, the caldera region near the northeast dome began to inflate, and accompanying surface uplift migrated to the southwest dome between September 1996 and June 1997. These deformation data are consistent with hydrothermal or magmatic fluid migration into and out of two sill-like bodies that are about 8 kilometers directly beneath the caldera.

Yellowstone National Park (Fig. 1) is famous for its numerous hydrothermal features and other natural wonders but is better known among earth scientists as the site of the world's largest restless caldera. Many earth scientists believe the park is the present-day terminus of the active Yellowstone hotspot. The hotspot track can be traced along a string of large calderas (*1*) to its origin ~16 million years ago in southeastern Oregon and northern Nevada. The three most recent caldera-forming events occurred during cataclysmic rhyolite ash-flow tuff eruptions during the past 2.1 million years in the Yellowstone region (*1, 2*). Yellowstone caldera, the youngest of the three (Fig. 1), formed ~630,000 years ago in an eruption (many times larger than any historic volcanic eruption) that ejected ~1000 km^3 of debris—about 1000 times the volume of magma erupted at Mount St. Helens in May 1980 (*1*). A subsequent episode of dominantly extrusive volcanism buried Yellowstone caldera under rhyolite lava flows from 150,000 to 70,000 years ago (*2*). Even though the last magmatic eruption occurred ~70,000 years ago, geologic and geophysical evidence suggests that a crustal magma reservoir beneath Yellowstone is maintained in a partly molten state by episodic intrusions of basaltic magma (*3*). Because another caldera-forming eruption is almost inevitable, though not imminent, a continuous monitoring program is important. It is equally important, however, to assess the patterns of deformation

C. Wicks Jr. and W. Thatcher, U.S. Geological Survey (USGS), MS 977, Menlo Park, CA 94025, USA. D. Dzurisin, USGS, Cascades Volcano Observatory, 5400 MacArthur Boulevard, Vancouver, WA 98661, USA.